Improvement of terahertz imaging with a dynamic subtraction technique

Zhiping Jiang, X. G. Xu, and X.-C. Zhang

By use of dynamic subtraction it is feasible to adopt phase-sensitive detection with a CCD camera to reduce long-term optical background drift. We report on a two-order improvement of the signal-to-noise ratio. The improved system is used to image terahertz field distribution generated by an optically rectified electro-optic crystal with a modulation depth as small as 10^{-4}. We also introduce a modified detection geometry that realizes near-field imaging capability with greatly improved spatial resolution.

OCIS codes: 320.7100, 110.2970, 320.7120, 250.5530.

1. Introduction

The accessibility of electromagnetic waves in the terahertz range has opened an avenue for scientific research as well as practical applications. The techniques of detecting terahertz pulses are mature for single-point measurement. However, there is still a need for fast two-dimensional (2D) measurement. First, terahertz imaging was originally realized by raster scanning of the object located at the focal plane.[1,2] The imaging speed is obviously limited by the scanning speed. Depending on the number of the pixels and the integral time it may take minutes or hours to get one imaging picture, so it is difficult to realize real-time imaging. Second, the propagation of terahertz pulses that have a few cycles has attracted both theoretical and experimental interest recently. Interesting results on terahertz phenomena, such as pulse shaping, Gouy phase shift, and superlumina, are reported.[3–8] However, terahertz detection involved in these experiments is based on single-point measurement; i.e., spatially only one point is measured at a time. If an image of 2D distribution is needed, it is necessary to scan the detecting system mechanically. This scanning is time consuming and not in real time. It is also difficult to keep the right timing between the pump beam and the probe beam. The lack of adequate experimental measurement prevents us from achieving deep insight into the complicated propagation of pulses with a few cycles.

Free-space electro-optic (EO) sampling provides an alternative method of measuring the terahertz electric field to photoconductive antenna. It has the advantages of easy alignment; wide bandwidth; high sensitivity; and, most importantly, the capability of parallel measurement. Wu *et al.*[9] and Lu *et al.*[10] proposed and demonstrated a 2D EO and CCD-based terahertz imaging system. This system takes advantage of the parallel measurement, and, in principle, the speed is limited only by the frame rate of the CCD camera. However, because the lock-in amplifier, which is used in the single-detector system and suppresses noise dramatically, cannot be used with the CCD camera, this system has poor signal-to-noise ratio (SNR). The improvement is imperative for extending the usefulness of such a terahertz system.

In this paper we report on the use of the dynamic subtraction technique (similar to phase-sensitive detection) during CCD data acquisition and processing. With this technique a modulation depth as small as 5×10^{-5} can be measured, and an improvement of SNR by approximately 2 orders is achieved. The principle and the setup are described in Section 2. Section 3 shows two examples of the application of this improvement. One application is to measure 2D electric field distributions of weak terahertz pulses generated by an optically rectified EO crystal;

Z. Jiang is with the Department of Physics, Applied Physics, and Astronomy, Rensselaer Polytechnic Institute, Troy, New York 12180-3590. X. G. Xu is with the Department of Environmental and Energy Engineering, Rensselaer Polytechnic Institute, Troy, N.Y. 12180-3590. X.-C. Zhang (zhangxc@rpi.edu) is with the Department of Physics, Applied Physics, and Astronomy and the Department of Electrical, Computer, and System Engineering, Rensselaer Polytechnic Institute, Troy, New York 12180-3590.

Received 15 January 2000; revised manuscript received 18 February 2000.

0003-6935/00/172982-06$15.00/0

another is for real-time terahertz imaging of a large object.

2. Principle and Setup

The operation principle is as follows: Assume that a small optical signal is carried on a large and noisy light background (in our case, a terahertz electric field induces small modulation on the probe beam inside the EO crystal). For the conventional measurement with a CCD a frame is first taken as the background picture without the signal; a consecutive frame is then taken with the signal. The difference between these two frames gives the signal picture. More frame accumulation increases SNR. Mathematically the signal S in the conventional CCD measurement can be written as

$$S = \frac{\sum_{n=1}^{N} I_n - \sum_{n=M+1}^{M+N} I_n}{\sum_{n=1}^{N} I_n + \sum_{n=M+1}^{M+N} I_n}, \qquad M > N, \tag{1}$$

where I_n is the nth frame. Obviously this method experiences long-term drift of the background. However, if the signal is modulated by a modulator (mechanical chopper or EO modulator), and the CCD is synchronized to the modulation frequency, it is possible to achieve phase-sensitive detection. Suppose that the even frames contain signal and background and that the odd frames contain background only; then the signal can be extracted dynamically from Eq. (2):

$$S = \frac{\sum_{n=1}^{N} (I_{2n} - I_{2n-1})}{\sum_{n=1}^{N} (I_{2n} + I_{2n-1})}. \tag{2}$$

Experimentally all the data (frames with signal on and off) are sent to a computer for the subtraction and the accumulation. Since the signal and the background frames are captured alternatively in the millisecond time scale, the long-term drift of the background is greatly reduced.

The experimental diagram of the terahertz imaging system is shown in Fig. 1. The frequency of the output synchronization signal NOTSCAN from the CCD camera (Roper's Pentamax with 384 × 288 pixels) is reduced by half to trigger the EO modulator. The laser pump beam, and therefore laser-induced terahertz radiation, is modulated synchronously with the CCD camera. The amplitude-modulated terahertz beam is then imaged onto a ZnTe EO crystal. The probe beam is expanded to cover the whole terahertz beam and propagates colinearly with the terahertz beam through the EO crystal. The polarization of the probe beam is modulated by the terahertz electric field through the EO effect. This polarization modulation is converted into intensity modulation by a polarization analyzer A with crossed polarization.[11] The CCD camera records the 2D

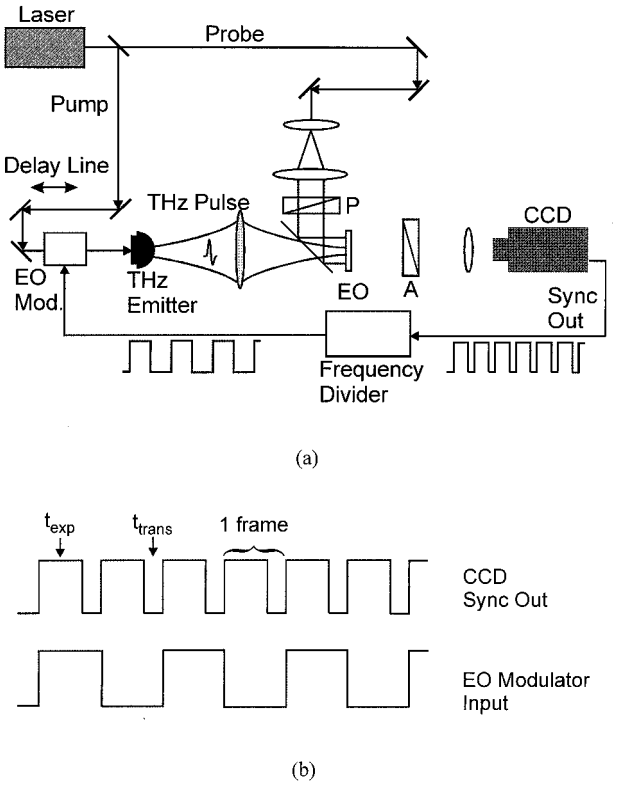

Fig. 1. (a) Experimental setup of terahertz imaging with dynamic subtraction, (b) timing diagram between the CCD output and the EO modulator trigger signals.

spatial distribution of the terahertz-modulated probe beam.

Since the noise floor is determined solely by the probe beam, the system is tested with the optical background only (without terahertz signal). In this case the EO crystal is replaced with a patterned target. Figures 2(a) and 2(b) show the typical noise pictures obtained with conventional subtraction and with dynamic subtraction, respectively. For a perfect subtraction in an ideal case the target pattern should be subtracted and average out completely. For 1000 frames of accumulation the rms noise with dynamic subtraction is ~100 times smaller than with conventional subtraction. The residual noise in Fig. 2(a) is random, whereas the noise in Fig. 2(b) shows a spatial pattern (such as grid and letters). This noise pattern (which is due to the long-term optical background drift) cannot be eliminated by conventional accumulation. In addition, because the time interval between the signal frame and the reference frame is smaller, even without averaging, dynamic subtraction still works well. The measured rms noise for 1000 dynamic subtractions is less than 0.2 counts, and the full dynamic range of the CCD camera is 12 bit; therefore it is possible to measure a modulation depth as small as $0.2/2^{12} \approx 5 \times 10^{-5}$. Figures 2(c) and 2(d) plot the images of terahertz pulse measured with dynamic subtraction (phase-sensitive method) and conventional subtraction, respectively. By comparison of Fig. 2(c) with Fig. 2(d),

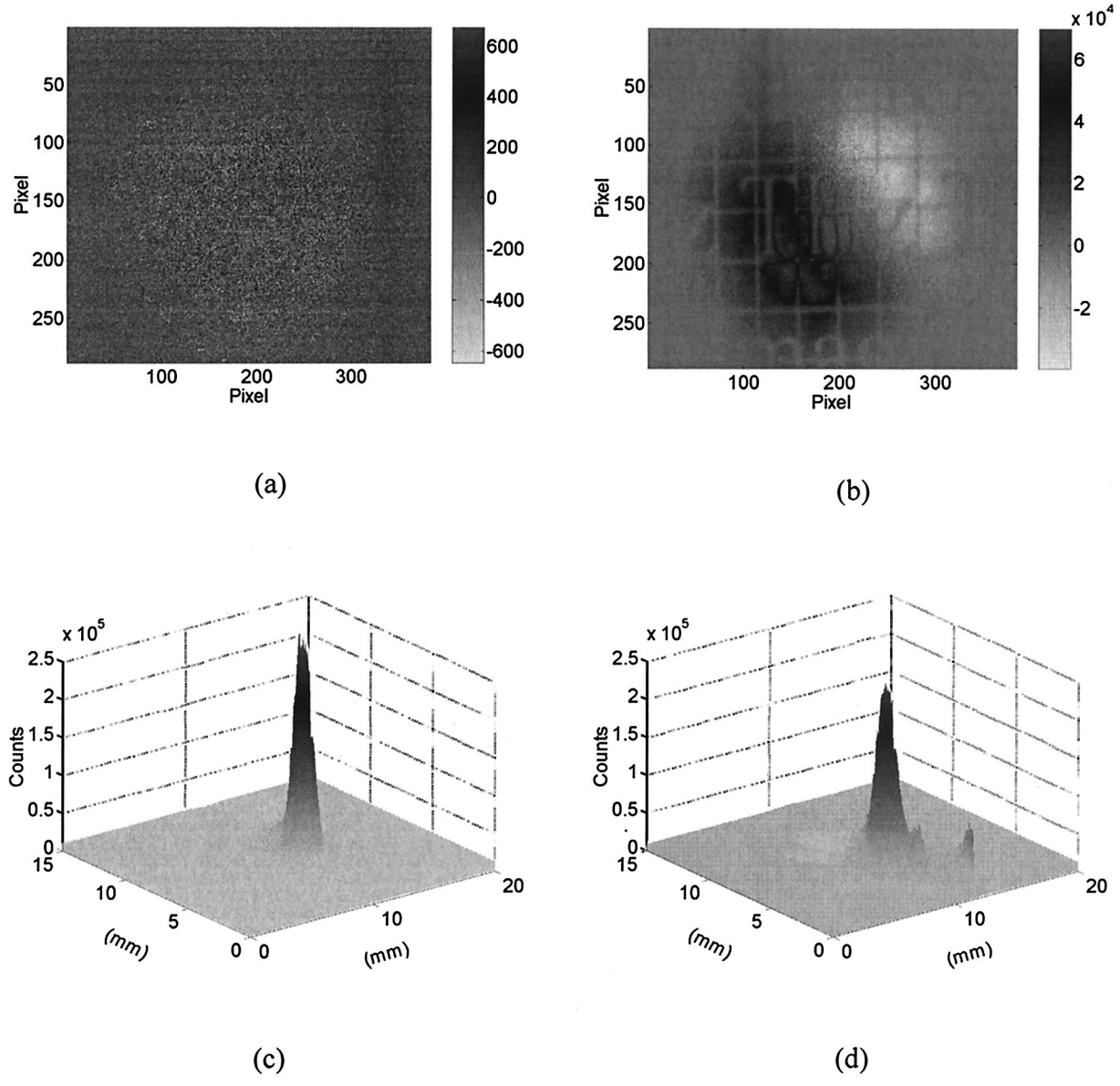

Fig. 2. Typical residual counts from a patterned target after 1000 averages with (a) dynamic subtraction and (b) conventional average. The rms counts are 0.15 and 24.0/frame for (a) and (b), respectively. 2D images of a terahertz field measured with (c) dynamic subtraction and (d) conventional subtraction.

it is easily seen that the background noise is greatly reduced with this phase-sensitive method [Fig. 2(c)]. The signal in Fig. 2(c) is higher than that in Fig. 2(d), because the polarization-modulation technique[12] is adapted.

3. Applications

With this improved sensitivity it is feasible to image a relatively weak terahertz electric field, which would be impossible without dynamic subtraction. One example shown here is the imaging of a terahertz field generated by optical rectification from an EO crystal. In this experiment the laser used is the Coherent Ti:sapphire amplifier RegA 9000, which produces pulses with 1-W average power, 250-fs pulse duration, 830-nm wavelength, and repetition rate of 250 kHz. The emitter is a 2-mm ⟨110⟩ ZnTe crystal with a silicon ball attached to it to collimate the radiation; the emitted terahertz beam is focused onto a 4-mm ⟨110⟩ ZnTe crystal by parabolic mirrors. The pixels of the detector array in the CCD camera are grouped by 2×2 to decrease the amount of data and therefore increase the speed. The exposure time used is 5 ms. With these parameters, a frame rate as high as 69 frames/s (FPS) is reached. 2D terahertz images at a frame rate greater than 30 FPS (faster than the video rate) can be obtained and displayed on the computer monitor. Figure 3(a) shows a peak electric field distribution. Figure 3(b) plots the temporal waveform at the center of the terahertz spot in Fig. 3(a). This is the direct measurement of a weak terahertz signal from the optical rectification emitter without a

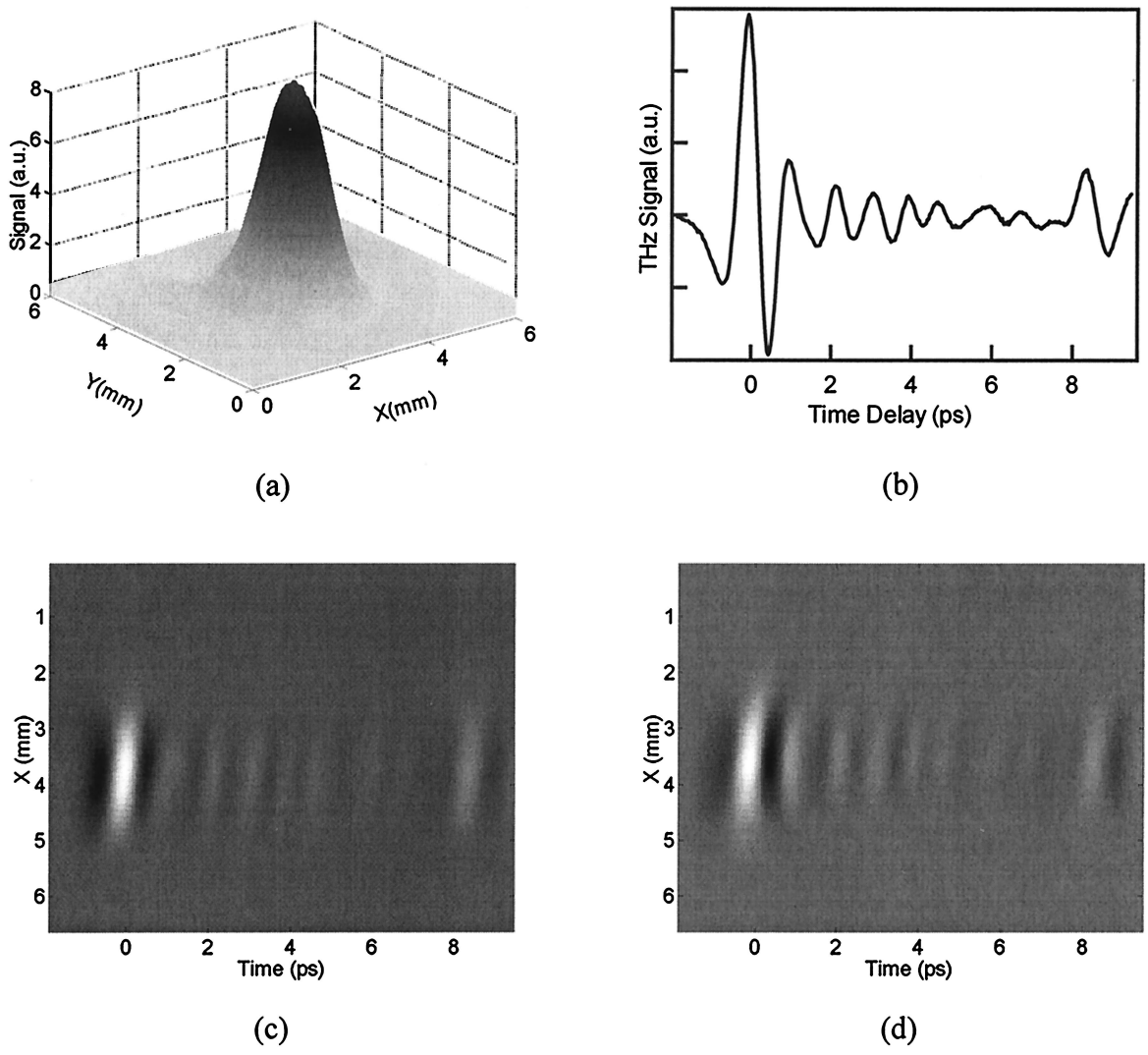

Fig. 3. Electric field distribution measured with dynamic subtraction from an optical rectification emitter. (a) 2D distribution at peak signal; (b) temporal waveform at the main peak; (c) and (d) 1D spatial and 1D temporal distribution at and 1.5 cm away from the focal plane, respectively.

lock-in amplifier. Figures 3(c) and 3(d) show one-dimensional (1D) spatial and 1D temporal field distributions at and 1.5 cm away from the focal plane, respectively. Rings after the main peak are clearly seen. Note that the wave fronts are different in Figs. 3(c) and 3(d). The wave front at the focal plane is planar [Fig. 3(c)], whereas the wave front at the defocal plane is curved [Fig. 3(d)], indicating that the terahertz beam is divergent. The slightly tilted wave front [Figs. 3(c) and 3(d)] is due to the small angle between the propagation direction of the terahertz beam and the probe beam.

By scanning the imaging crystal along the z axis (the terahertz propagation direction) while keeping the terahertz-probe timing at the main peak position, we obtain the xz field distribution, as shown in Fig. 4. This figure displays the field pattern at and away from the focal plane.

We made several movies, showing the dynamic evolution of terahertz pulses. We also used this system to monitor the terahertz spot during alignment in real time. The perfect alignment of four parabolic mirrors is not a trivial job, especially for the invisible terahertz beam. Since we could see the terahertz beam at this point, we twisted the parabolic mirrors while watching the terahertz spot on the computer monitor to optimize the terahertz spot, and therefore to optimize the alignment. We corrected the focused spot from elliptical to nearly round one with increased electric field at the beam center.

Another example given here is real-time terahertz imaging. Since we have much better SNR, we can either expand the terahertz beam to image a larger object or increase the display speed. To get real-time imaging, an expanded terahertz beam is needed. Therefore an externally biased large-aperture photoconductive antenna was used to obtain as much terahertz power as possible. The central frequency of the terahertz pulses generated by this kind of large-aperture photoconductive antenna is very low, less

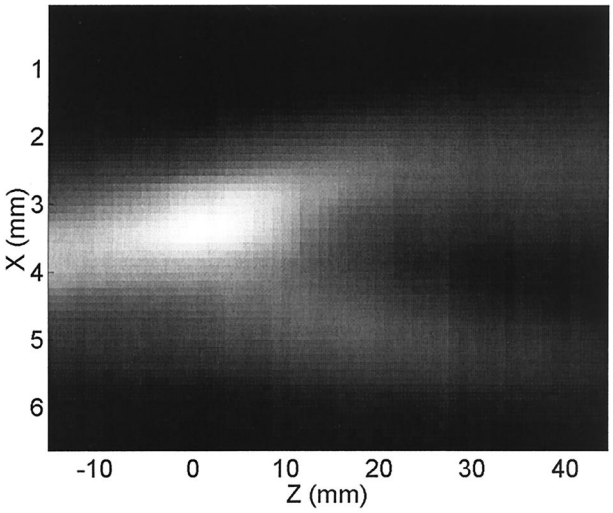

Fig. 4. Electric field distribution of terahertz pulse in *xz* plane at time zero.

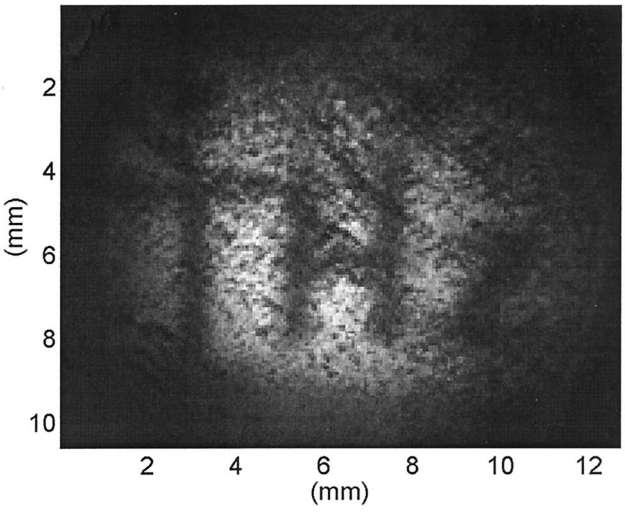

Fig. 6. Terahertz imaging of a mask with three letters THz taken by the near-field geometry in Fig. 5 and the dynamic subtraction technique in Fig. 1.

than 0.3 THz. To have reasonable spatial resolution, a modified EO terahertz imaging system was used instead of the 2*f*–2*f* imaging system. As shown in Fig. 5, the probe beam is reflected at the front surface of the EO crystal and then propagates with the terahertz beam colinearly inside the crystal. In this way the object can be placed close to or even in touch with the EO crystal. If the object under imaging is thin, near-field terahertz imaging is realized with greatly improved spatial resolution. It has been proved experimentally as well as theoretically that the terahertz waveform measured in this reflection geometry is the same as that in the transmission geometry. The reason is that the contribution from the part of counterpropagation is negligible. We used a mask with three letters, THz. Fig. 6 shows the imaged result. The spatial resolution is improved by at least 5 times compared with that in the 2*f*–2*f* imaging system, and the image can be displayed on the computer screen in real time.

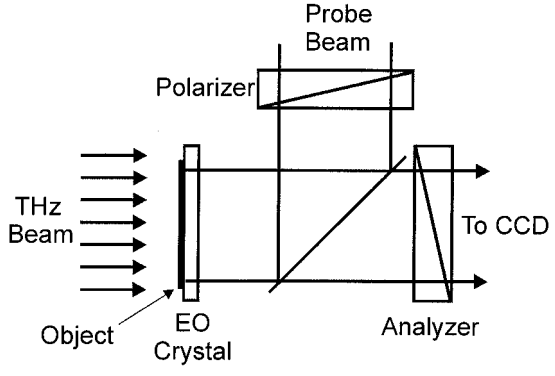

Fig. 5. Near-field 2D terahertz imaging. The probe beam is reflected by the EO crystal at the surface facing the object; therefore the object can be located close to the EO crystal without blocking the probe beam.

4. Conclusions

The EO imaging technique with dynamic subtraction provides a unique method to visualize the spatial distribution of a 2D terahertz electric field and for real-time imaging. With real-time display capability (greater than 30 FPS) it has been used to track and monitor the terahertz beam path and distribution in the terahertz imaging system. Once a pulsed terahertz beam has only a few cycles (even a single cycle in certain cases), it undergoes strong pulse shaping during the propagation. The temporal waveform strongly depends on the spatial position. This imaging system is an ideal system to characterize the time-dependent diameter and wave front of a terahertz beam distribution. A video of terahertz imaging with several different propagating geometries is taken, and these results will be reported elsewhere.

In conclusion, the performance of a 2D CCD-based terahertz imaging system has been improved by 2 orders with use of the phase-sensitive detection. The parallel measurement capability and high sensitivity make this imaging system a unique tool for visualizing a 2D terahertz field distribution in real time. The distribution of a weak terahertz field by optical rectification in EO crystal is measured. The current dynamic subtraction rate is 69 FPS. By larger-area pixel binning in the CCD camera and by software modification, it is possible to increase the subtraction rate from 69 to 300 PFS. With this high-speed dynamic subtraction (300 FPS) we expect that the signal-to-noise ratio (SNR) of a 2D terahertz image with a large dynamic range CCD (18 bit or higher) may be close to that in the single-point measurement with a lock-in amplifier.

Part of this research was supported by the U.S. Army Research Office and the U.S. Department of Energy.

References

1. B. B. Hu and M. C. Nuss, "Imaging with terahertz waves," Opt. Lett. **20,** 1716–1718 (1995).
2. D. M. Mittleman, R. H. Jacobsen, and M. C. Nuss, "T-ray imaging," IEEE J. Sel. Top. Quantum Electron. **2,** 679–692 (1996).
3. A. E. Kaplan, "Diffraction-induced transformation of near-cycle and subcycle pulses," J. Opt. Soc. Am. B **15,** 951–956 (1999).
4. D. You and P. H. Bucksbaum, "Propagation of half-cycle far infrared pulses," J. Opt. Soc. Am. B **14,** 1651–1655 (1997).
5. S. Feng, H. G. Winful, and R. W. Hellwarth, "Gouy shift and temporal reshaping of focused single-cycle electromagnetic pulses," Opt. Lett. **23,** 385–387 (1998); errata **23,** 1141 (1998).
6. Z. L. Horvath, J. Vinko, Z. Bor, and D. von der Linde, "Acceleration of femtosecond pulses to superluminal velocities by Gouy phase shift," Appl. Phys. B **63,** 481–484 (1996).
7. S. Hunsche, S. Feng, H. G. Winful, A. Leitenstorfer, M. C. Nuss, and E. P. Ippen, "Spatiotemporal focusing of single-cycle light pulses," J. Opt. Soc. Am. A **16,** 2025–2028 (1999).
8. K. Wynne and D. A. Jaroszynski, "Superluminal terahertz pulses," Opt. Lett. **24,** 25–27 (1999).
9. Q. Wu, T. D. Hewitt, and X.-C. Zhang, "Two-dimensional electro-optic imaging of THz beams," Appl. Phys. Lett. **69,** 1026–1028 (1996).
10. Z. G. Lu, P. Campbell, and X.-C. Zhang, "Free-space electro-optic sampling with a high-repetition-rate regenerative amplified laser," Appl. Phys. Lett. **71,** 593–595 (1997).
11. Z. Jiang, F. G. Sun, Q. Chen, and X.-C. Zhang, "Electro-optic sampling near zero optical bias point," Appl. Phys. Lett. **74,** 1191–1193 (1999).
12. Q. Chen and X.-C. Zhang, "Polarization modulation in optoelectronic generation and detection of terahertz beams," Appl. Phys. Lett. **74,** 3435–3437 (1999).